Proceedings World Geothermal Congress 2026
Calgary, Canada, June 8 – 11, 2026

Calabozos Hydrothermal System: An Approach from Petrology and Geochemistry of Hydrothermal Alteration

Villarroel M[1]*, Morata D[1] and Maza S[1] and Ruprecht P[2]
Departamento de Geología & Centro de Excelencia en Geotermia de Los Andes (CEGA), Facultad de Ciencias Físicas y Matemáticas, Universidad de Chile, Santiago, Chile[1]
Department of Geological Sciences and Engineering, University of Nevada, Reno, United States[2]
zulay.villarroel@ug.uchile.cl*

1. INTRODUCTION

As global efforts to mitigate climate change accelerate, the demand for sustainable, low-carbon, and renewable energy sources has increased significantly. Geothermal energy has gained particular attention due to its capacity for continuous, base-load power generation and its ability to provide a reliable alternative to fossil fuel-based energy systems. Geothermal resources are commonly found in tectonically active and volcanic regions due to the high geothermal gradient. In these regions upward heat flux along faults produces surface manifestations such as thermal springs (Limberger et al., 2018; Moeck, 2014). Nearly 75% of productive and prospective geothermal power plants worldwide are associated with subduction-zone volcanoes (Moeck, 2014).

Among volcanic centers, calderas hosting hydrothermal systems are prime candidates for geothermal energy resources. According to Stelling et al. (2016), out of 74 global arc-related volcanic centers hosting power-producing geothermal systems, approximately 60% are associated with calderas. Hydrothermal systems hosted on calderas are characterized by the accumulation and circulation of fluids through fracture networks within the caldera, typically above the crystallizing magma reservoir, and often partially confined by impermeable layers such as clays or welded tuffs (Giordano & Cas, 2024; Goeff & Gardner, 1994). Surface manifestations of these systems include hot springs, geysers, fumaroles, and mud pools. The circulating fluids cause chemical and mineralogical alterations in the caldera floor and margins, creating distinct alteration zones (argillic, propylitic, and phyllic) that vary with depth and temperature. These hydrothermal systems can persist long after caldera forming eruptions, leading to the mobility of alkali and silica and the development of alteration assemblages, including sericite, epidote, and carbonate (Wright et al., 2024).

2. GEOLOGICAL SETTING

The Chilean Andes, characterized by extensive volcanic and tectonic activity, host some of the world's most promising but underutilized geothermal resources. Among these, the Calabozos Caldera Complex (CCC) is a high-potential geothermal system due to its recent magmatic history, structural complexity, and outstanding hydrothermal activity. However, despite its potential, the CCC remains largely unexplored. No comprehensive geothermal model integrating surface and subsurface data has been developed. The Calabozos Caldera Complex (35° 30' S, 70° 37' W), defined by Hildreth et al. (1981) is a silicic volcanic center in the Maule Region of Chile (Figure 1). It formed in the backarc of several Pleistocene to Holocene volcanic centers of the Andean Arc (e.g. Descabezado Grande, Planchon Peteroa). The caldera floor is 2600 meters above sea level (m.a.s.l.), while its eastern wall and central uplift reach 3000 m.a.s.l. (Hildreth et al., 1984).

Hildreth et al. (1984) conducted the first detailed mapping of the caldera, which revealed a caldera extent of 26 km x 14 km. It was proposed to represent a trap-door collapse caldera formed in a series of three major eruptive events, classified by age and volume: Unit L (0.8 Ma, 500 km^3), Unit V (0.3 Ma, 350 km^3), and Unit S (0.15 Ma, 200 km^3) (Hildreth et al., 1984). These Late Pleistocene ignimbrites of erupted dacite to rhyodacite (Grunder, 1987; Hildreth et al., 1984) are commonly collectively named the Loma Seca Tuff. They correspond to 95% of the volume erupted by the CCC.

In the case of the CCC, thermal manifestations are a notable feature. There are eight thermal springs in the area with surface temperatures reaching up to 94°C (Benavente et al., 2016). It has been estimated that it has probably persisted for 300,000 years or more, which may suggest the existence of a geothermal reservoir at depth (Grunder et al., 1987). Grunder et al. (1987) characterized the CCC hydrothermal system, emphasizing the strong tectonic-structural control on fluid upflow. They identified two principal hydrothermal discharge zones: 1) along a fault surrounding the resurgent uplift within the caldera and 2) at the southwestern margin of the caldera (Figure 1). Finally, in 2009, the National Geothermal Company S.A. drilled the Llolli-01 well in the Vegas de Pangal area (35° 22' S, 70° 35' W) at an altitude of 1750 m.a.s.l., reaching a depth of 901 m (Figure 2). The well's temperature profile recorded 182°C at a depth of 889 m (Rivera et al., 2009).

Building on this previously published data, this project aims to develop a conceptual model of the CCC geothermal system by integrating surface and subsurface data to characterize its geothermal potential. The first objective will focus on analyzing the hydrothermal alteration of the Llolli-01 drill core to determine stratigraphic sequences and alteration mineral facies, providing insights into reservoir conditions.

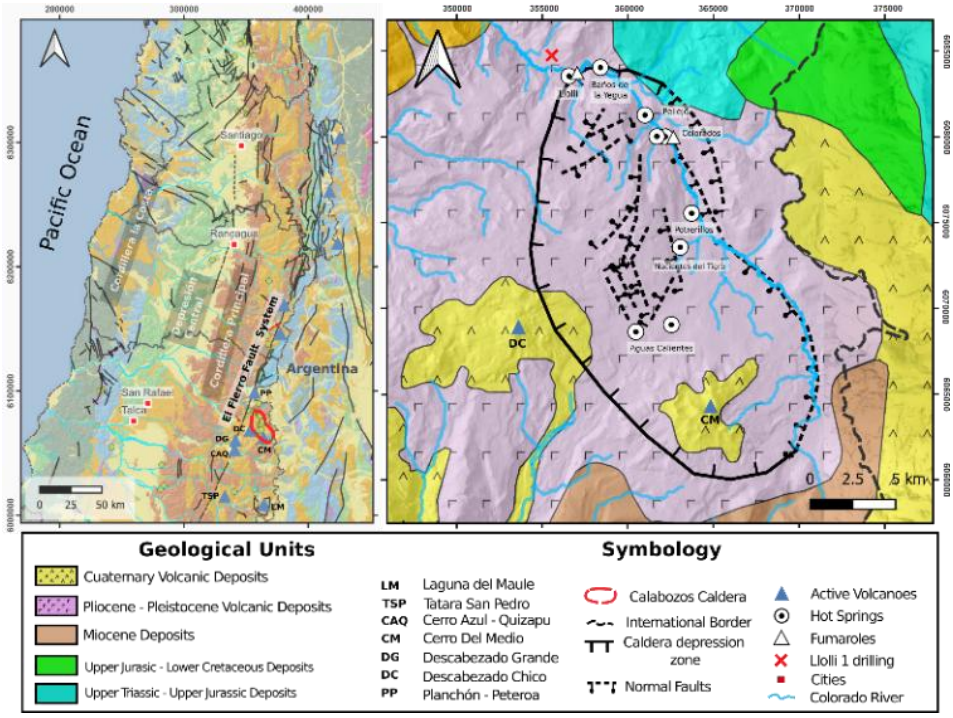


Figure 1. Regional location of the Calabozos Caldera Complex with its most notable geological features (based on: Grunder et al., 1987; Tapia, 2010).

3. METHODS & RESULTS

The mineralogical and geochemical characterization of hydrothermal alteration was carried out using whole-rock X-ray diffraction (XRD) analysis. Drill core Llolli-01 was systematically sampled at 10 m intervals, ensuring representation of the different geological units identified along the sequence (Figure 2). Both host-rock and vein samples were prepared for XRD analysis, selecting a representative sample for each lithology.

For whole-rock XRD sample preparation, the material was ground in an agate mortar to a grain size of < 50 µm. The powdered samples were then mounted onto sample holders and analyzed using a Bruker D2 PHASER diffractometer (CEGA, Department of Geology, Universidad de Chile) equipped with a CoKα radiation source (1.78897 Å). The analytical conditions were set to 30 kV and 10 mA, with a scanning range of 5°–80° 2θ, step size of 0.006°, and step time of 0.95 s. Mineral identification from the resulting diffractograms was performed using Diffrac.EVA V5.2 software, while mineral phase quantification was carried out through Rietveld refinement using TOPAS 6 and the Crystallography Open Database. Furthermore, Scanning Electron Microscopy equipped with Energy Dispersive X-Ray spectroscopy (SEM-EDX) was performed at the University of Nevada, Reno (USA), to document the main hydrothermal textures and hydrothermal assemblages in polished thin sections from the most representative samples of the drill core (Figure 3).

The lithological sequence of the drill hole (Figure 2) reveals an initial interval of unconsolidated sediments (0–21 m), followed by a thick evaporitic succession (21–420 m) dominated by anhydrite, interbedded with sandstones, conglomerates, and volcanic rocks belonging to the Nacientes del Teno Formation (Jurassic). Between 420 and 640 m, a sequence of tuffs, lapilli, and breccias from the Coya-Machalí Formation (Paleogene) was identified. From 640 to 901 m, alternating carbonate, clastic, andesitic, and quartz-bearing microdioritic units occur (Jurassic). Structural evidence suggests the presence of a reverse fault that brings the older Jurassic strata to shallower levels, placing the younger volcanic sequence in the middle of the drill core stratigraphy. Additionally, andesitic lava intrusions are observed mainly within the Jurassic units.

The mineralogical analysis of hydrothermal alteration within the first 500 m indicates a predominance of phyllosilicates (illite, chlorite, and montmorillonite), zeolites (laumontite), carbonates (calcite, dolomite, ankerite, and siderite), epidote (clinozoisite), and sulfates (anhydrite) (Figure 2). Modal and compositional

variations are closely related to lithological changes, with anhydrite and calcite being the primary mineral phases filling veinlets (Figure 3). In contrast, clinozoisite and chlorite are abundant within the andesitic lava intrusions around the 300 m depth level. In the sample from 213.72 m, chlorite is observed replacing plagioclase crystals, whereas in the 317.30 m sample, chlorite occurs along the edges of the main calcite–anhydrite veins, showing Fe enrichment.

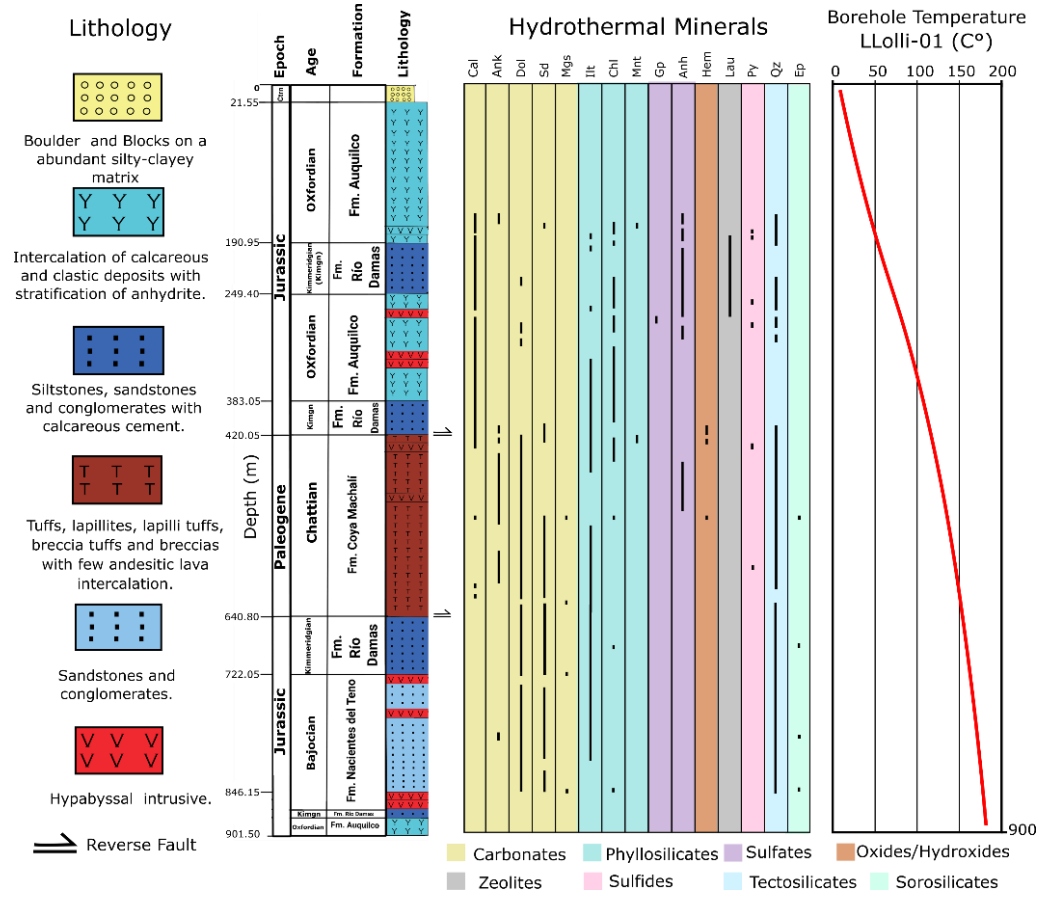


Figure 2. Lithological column of the Llolli-1 borehole and spatial distribution of hydrothermal minerals. The temperature profile of the Llolli-01 exploratory well shows the trend of the maximum temperatures measured and inferred through thermometry (red line), according to data reported by ENG (Rivera et al., 2009). Mineral abbreviations: Cal: calcite; Ank: ankerite; Dol: dolomite; Sd: siderite; Mgs: magnesite; Ilt: illite; Chl: chlorite; Mnt: montmorillonite; Gp: gypsum; Anh: anhydrite; Hem: hematite; Lau: laumontite; Py: pyrite; Qz: quartz; Ep: epidote.

At the same depth, clinozoisite appears as partial replacement of plagioclase and amphibole phenocrystals. In the shallow volcanic levels, the alteration assemblage consists of calcite, laumontite, chlorite, albite, and quartz. In contrast, deeper intervals (> 420 m) are characterized by illite, dolomite, and siderite, with minor smectite (Figure 2). Vein fillings are mainly composed of quartz and Mg–Fe–rich carbonates such as ankerite and dolomite (Figure 3c, 3d). In these levels, albitization is locally observed along vein margins, and the matrix of the sedimentary units is pervasively altered to illite.

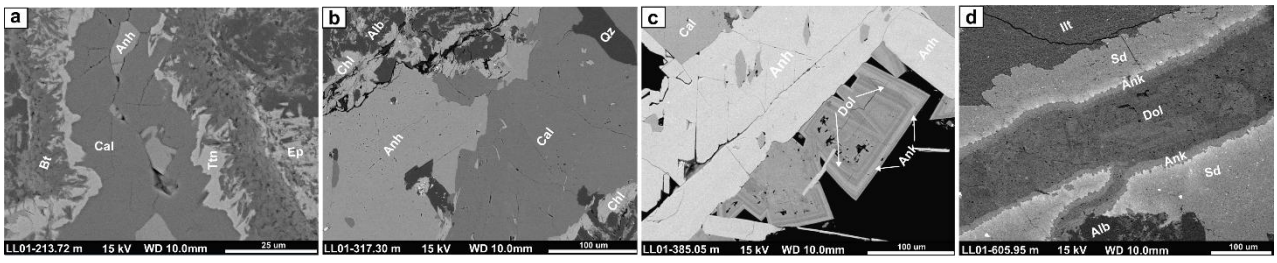


Figure 3. SEM figures of microphotographs of alteration veins found on the drill core Llolli-01. Mineral abbreviations: Cal: calcite; Ank: ankerite; Dol: dolomite; Sd: siderite; Chl: chlorite; Anh: anhydrite; Qz: quartz; Ep: epidote; Alb: albite; Bt: biotite; Ttn: titanite; Msc: muscovite; Ilt: illite.

SEM analyses reveal notable textural variations in hydrothermal veins along the drill core. The vein at 213.72 m consists predominantly of calcite, with minor anhydrite growth in the center, forming a crustiform texture and surrounded by micaceous minerals (Figure 3a). The vein at 317.30 m exhibits a greater anhydrite content and minor quartz, displaying a jigsaw texture, bordered by Fe-rich chlorite (clinochlore) (Figure 3b). The vein at 385.05 m is dominated by anhydrite, displaying a lattice-bladed texture, and is intergrown with zoned rhombohedral carbonates that alternate between Mg-rich dolomite and Fe-rich ankerite (Figure 3c). In the deeper sections, particularly at 605.00 m, the veins are dominated by Mg–Fe carbonates, showing crustiform intergrowths of dolomite, ankerite, and siderite (Figure 3d). From this depth downward, the quartz content in the veins increases noticeably.

4. DISCUSSION

The mineral distribution and paragenetic associations indicate the interaction between the evaporitic–volcanic sequence and ascending geothermal fluids, where structural control plays a key role in the observed alternation of lithologies (Figure 2). Along the core, at least two hydrothermal alteration zones can be distinguished. The assemblage of calcite, laumontite, chlorite, and quartz, identified in the upper intervals, suggests near-neutral pH conditions, high Ca availability, and temperatures around 180 °C, consistent with low-sulfidation, chloride-dominated hydrothermal fluids producing propylitic alteration. In deeper sections, the dominance of illite associated with Fe- and Mg-rich carbonates reflects intermediate argillic alteration, distributed more pervasive along the core and indicative of temperatures near 200 °C, higher K content, and fluid compositions typical of longer residence times within the geothermal system. The observed textural variations in hydrothermal veins along the Llolli-1 drill core reflect fluctuating physicochemical conditions during vein formation, primarily controlled by temperature, fluid composition, and crystallization rate.

The crustiform texture of calcite and anhydrite observed at shallow levels (Figure 3a) suggests episodic vein opening and mineral precipitation from low-temperature fluids under fluctuating supersaturation, a characteristic feature of near-surface hydrothermal environments (Dong et al., 1995; Moncada et al., 2012). At intermediate depths (317.30–385.05 m), the transition to jigsaw and lattice-bladed textures, accompanied by Fe-rich chlorite and zoned carbonates, indicates periodic fluid boiling and rapid pressure fluctuations, promoting simultaneous crystallization of carbonates, sulfates, and silicates (Figure 3b, 3c) (Bodnar et al., 1985; Henley and Ellis, 1983). Besides, the presence of Mg–Fe carbonates intergrown with anhydrite is consistent with higher-temperature and more reducing conditions, where Fe–Mg exchange between carbonates and silicates becomes more efficient (Pirajno, 2009; Reed, 1997). At a depth of 605.65 m, the presence of crustiform textures alternating between Fe- and Mg-rich carbonates records variations in redox conditions during vein formation, indicating dynamic fluctuations in the chemical environment of the hydrothermal system. In contrast, the progressive increase in quartz content below 600 m suggests a transition toward silica-saturated fluids and intensified fluid–rock interaction**,** indicating a well-defined thermal and chemical gradient within the system.

5. CONCLUSIONS

The mineralogical and textural variations observed along the Llolli-1 drill core of the CCC record the progressive evolution of hydrothermal activity, from shallow, low-salinity fluids to deeper, chemically equilibrated geothermal conditions. The presence of distinct alteration zones, the progressive enrichment in quartz, and the development of Fe–Mg carbonate assemblages at depth indicate a well-defined thermal gradient and dynamic fluid–rock interaction within the system. Furthermore, the presence of illite and smectitic clays suggests the formation of a clay cap-rock layer, consistent with a conductive geothermal regime and the potential existence of a deeper reservoir beneath the Calabozos Caldera Complex. The temperature profile measured during drilling further supports this interpretation, suggesting that the evaporitic sequence may function as an effective hydrothermal seal, trapping heat at depth and enhancing the overall thermal retention capacity of the system.

Acknowledgements

This research was funded by the Agencia Nacional de Investigación y Desarrollo (ANID) Doctoral Scholarship (Folio: 21241398), with additional support from the Centro de Excelencia en Geotermia de los Andes (CEGA), the Anillo Project “The Water-Energy-Food Nexus for Urban Areas in Central Chile (WEF-Chile)” ATE220029, and the Subduction Zones in Four Dimensions (SZ4D) USA–Chile Exchange Initiative. The author acknowledges the University of Nevada, Reno, and its Department of Geological Sciences and Engineering for providing laboratory facilities that supported the analytical work of this study.

REFERENCES

Benavente, O., Tassi, F., Reich, M., Aguilera, F., Capecchiacci, F., Gutiérrez, F., Vaselli, O., and Rizzo, A.: Chemical and isotopic features of cold and thermal fluids discharged in the Southern Volcanic Zone

between 32.5°S and 36°S: Insights into the physical and chemical processes controlling fluid geochemistry in geothermal systems of Central Chile, Chemical Geology, **420**, (2016), 97–113.

Bodnar, R., Reynolds, T. J., and Kuehn, C. A.: Fluid inclusion systematics in epithermal systems, in Berger, B.R., and Bethke, P.M., eds., Geology and Geochemistry of Epithermal Systems. Reviews in Economic Geology, **2**, (1985), 73–97.

Dong, G., Morrison, G., and Jaireth, S.: Quartz textures in epithermal veins, Queensland; classification, origin and implication, Economic Geology, **90(6)**, (1995), 1841–1856.

Giordano, G., Cas, R., and W. J. V.: The Geology of Volcanoes and Their Facies Models. In Volcanology: Processes, Deposits, Geology and Resources, (2024),1239–1426.

Goeff, F., and Gardner, J. N.: Evolution of a mineralized geothermal system, Valles Caldera, New Mexico. Economic Geology, **89(8)**, (1994), 1803–1832.

Grunder, A.: Low $\delta^{18}O$ silicic volcanic rocks at the Calabozos caldera complex, southern Andes: Evidence for upper-crustal contamination, Contributions to Mineralogy and Petrology, **95(1)**, (1987), 71–81.

Grunder, A., Thompson, J., and Hildreth, W.: The hydrothermal system of The Calabozos Caldera, Central Chilean Andes, Journal of Volcanology and Geothermal Research, **32(4)**, (1987), 287–298.

Henley, R. W., and Ellis, A. J.: Geothermal systems ancient and modern: a geochemical review, Earth-Science Reviews, **19(1)**, (1983), 1–50.

Hildreth, W., Drake, R. E., and Sharp, W. D.: Voluminous late Pleistocene ash-flow and caldera complex in the Andes of Central Chile. Geological Society of America Abstracts with Programs, **13**, (1981), 61.

Hildreth, W., Grunder, A., and Drake, R.: The Loma Seca tuff and the Calabozos caldera: a major ash-flow and caldera complex in the southern Andes of central Chile, Geological Society of America Bulletin, **95(1)**, (1984), 45–54.

Limberger, J., Boxem, T., Pluymaekers, M., Bruhn, D., Manzella, A., Calcagno, P., Beekman, F., Cloetingh, S., and van Wees, J. D.: Geothermal energy in deep aquifers: A global assessment of the resource base for direct heat utilization, Renewable and Sustainable Energy Reviews, **82**, (2018), 961–975.

Moeck, I. S.: Catalog of geothermal play types based on geologic controls, Renewable and Sustainable Energy Reviews, **37**, (2014), 867–882.

Moncada, D., Mutchler, S., Nieto, A., Reynolds, T., Rimstidt, J., and Bodnar, R.: Mineral Textures and Fluid Inclusion Petrography of the Epithermal Ag-Au Deposits at Guanajuato, Mexico: Application to Exploration, Journal of Geochemical Exploration, **114**, (2012), 20–35.

Pirajno, F.: Hydrothermal Processes and Wall Rock Alteration, In: Hydrothermal Processes and Mineral Systems, Springer, (2009), 73-164.

Reed, M. H.: Hydrothermal Alteration and Its Relationship to Ore Fluid Composition. In Geochemistry of Hydrothermal Ore Deposits, **3**, (1997), 303–366.

Rivera, G., Ramírez, C., Vidal, A., and González, M.: Informe técnico: Proyecto Calabozo, Informe final pozo Llolli 1, Empresa Nacional de Geotermia Nacional S.A., (2009).

Stelling, P., Shevenell, L., Hinz, N., Coolbaugh, M., Melosh, G., and Cumming, W.: Geothermal systems in volcanic arcs: Volcanic characteristics and surface manifestations as indicators of geothermal potential and favorability worldwide, Journal of Volcanology and Geothermal Research, **324**, (2016), 57–72.

Tapia, F.: Análisis estructural del sector occidental de la faja plegada y corrida de Malargüe en el curso superior del río Colorado de Lontué (35°18' y 35°23'S), Región del Maule, Chile, Memoria para optar al Título de Geólogo, Universidad de Chile, (2010), 13.

Wright, J. V., Cas, R., and Giordano, G.: Volcanic-Hosted Resource, In Volcanology: Processes, Deposits, Geology and Resources, (2024), 1591–1797.